Acta Pharmacologica Sinica

www.nature.com/aps

ARTICLE

STING inhibitor ameliorates LPS-induced ALI by preventing vascular endothelial cells-mediated immune cells chemotaxis and adhesion

Bing Wu[1,2], Meng-meng Xu[1,3], Chen Fan[1], Chun-lan Feng[1], Qiu-kai Lu[1,2], Hui-min Lu[1,2], Cai-gui Xiang[1,2], Fang Bai[1,2], Hao-yu Wang[1,2], Yan-wei Wu[1] and Wei Tang[1,2]

Acute lung injury (ALI) is a common and devastating clinical disorder featured by excessive inflammatory responses. Stimulator of interferon genes (STING) is an indispensable molecule for regulating inflammation and immune response in multiple diseases, but the role of STING in the ALI pathogenesis is not well elucidated. In this study, we explored the molecular mechanisms of STING in regulating lipopolysaccharide (LPS)-induced lung injury. Mice were pretreated with a STING inhibitor C-176 (15, 30 mg/kg, i.p.) before LPS inhalation to induce ALI. We showed that LPS inhalation significantly increased STING expression in the lung tissues, whereas C-176 pretreatment dose-dependently suppressed the expression of STING, decreased the production of inflammatory cytokines including TNF-α, IL-6, IL-12, and IL-1β, and restrained the expression of chemokines and adhesion molecule vascular cell adhesion protein-1 (VCAM-1) in the lung tissues. Consistently, in vitro experiments conducted in TNF-α-stimulated HMEC-1cells (common and classic vascular endothelial cells) revealed that human STING inhibitor H-151 or STING siRNA downregulated the expression levels of adhesion molecule and chemokines in HMEC-1cells, accompanied by decreased adhesive ability and chemotaxis of immunocytes upon TNF-α stimulation. We further revealed that STING inhibitor H-151 or STING knockdown significantly decreased the phosphorylation of transcription factor STAT1, which subsequently influenced its binding to chemokine CCL2 and adhesive molecule VCAM-1 gene promoter. Collectively, STING inhibitor can alleviate LPS-induced ALI in mice by preventing vascular endothelial cells–mediated immune cell chemotaxis and adhesion, suggesting that STING may be a promising therapeutic target for the treatment of ALI.

Keywords: acute lung injury; STING; vascular endothelial cells; inflammatory cytokines; chemokines; chemotaxis

Acta Pharmacologica Sinica (2022) 43:2055–2066; https://doi.org/10.1038/s41401-021-00813-2

INTRODUCTION

Acute lung injury (ALI) and acute respiratory distress syndrome (ARDS) are common critical illnesses in clinical anesthesia and the intensive care unit [1–4]. These conditions are characterized by the accumulation of macrophages, neutrophils, alveolar-capillary membrane barrier dysfunction/disruption, and inflammatory factors production that frequently results in acute hypoxic respiratory insufficiency or failure. Sepsis and hemorrhagic shock remain the primary risk factors for the development of ALI/ARDS [3, 5, 6]. Despite great efforts that have been made in clinical care, ARDS continues to carry a high mortality rate [5, 6]. The molecular mechanisms responsible for the development of this are poorly understood, as well as therapeutic strategies targeting specific cytokines have not been effective in reducing the ARDS risk or mortality from sepsis [7, 8]. It is therefore of utmost importance to gain a deeper understanding of the underlying pathological mechanisms of ALI and develop novel therapeutic strategies for patients with ALI.

The endothelium is an important part in homeostasis of body physiology to safeguard transport logistics, control vascular permeability, and regulate vascular tone [9, 10]. At the same time, as an active part of the immune system, endothelial cells not only function as a transport device for immune cells and constitute a mechanical barrier against intruders, but they also have an essential paracrine function by expressing adhesion molecules and chemokines to organize recruitment of immune cells and regulate leukocyte extravasation at places of inflammation [9, 11]. Pro-inflammatory mediators such as TNF-α and/or IL-1β increase the production of multiple chemokines and adhesion molecules vascular cell adhesion protein (VCAM)-1 and intercellular adhesion molecule (ICAM)-1 on the surface of endothelial cells, which are essential for monocytes and polymorphonuclear neutrophils (PMN) rolling, adhesion, and migration [12]. Sustained activation of endothelium leads to massive infiltration of monocytes and PMNs, tissue damage, and organ dysfunction in the end [13]. Therefore, regulating the activation of endothelial cells may be a new direction for treating inflammatory diseases. However, the regulatory mechanisms of endothelial cells activation in ALI have not been fully elucidated.

[1]Laboratory of Anti-inflammation, Shanghai Institute of Materia Medica, Chinese Academy of Sciences, Shanghai 201203, China; [2]School of Pharmacy, University of Chinese Academy of Sciences, Beijing 100049, China and [3]School of Chinese Materia Medica, Nanjing University of Chinese Medicine, Nanjing 210000, China
Correspondence: Yan-wei Wu (wuyanwei@simm.ac.cn) or Wei Tang (tangwei@simm.ac.cn)

Received: 16 September 2021 Accepted: 1 November 2021
Published online: 14 December 2021

The stimulator of interferons genes (STING, also known as MITA, MPYS, and encoded by *Tmem173*) is an adapter protein involved in the immune response to cyclic dinucleotides that are produced by bacteria or metabolized from double-stranded DNA (dsDNA) by cyclic guanosine monophosphate-adenosine synthase (cGAS) and monophosphate [14–16]. Structurally, STING forms a complex with the TANK-binding kinase 1 (TBK1) to enable its phosphorylation, which results in activation of both interferon regulatory factor 3 and nuclear factor-κB, leading to the consequent production of type I interferons (IFNs) and inflammatory cytokines [17]. Increasing evidence suggests that impairment of the STING pathway has been associated with the pathogenesis of several diseases, including infections, inflammatory, and autoimmune diseases [18, 19].

The emerging role of cGAS-STING in sepsis or ALI has been revealed by several recent studies. Li et al. found that mt-DNA in cytosol and c-Myc cooperatively activated and upregulated STING, which subsequently led to LPS-induced ALI by promoting NOD-, LRR-, and pyrin domain-containing 3 (NLRP3) inflammasome and pyroptosis of macrophages. This study provided promising evidence for the targeting of STING-NLRP3 against ALI [20]. Joshi et al. demonstrated an essential role of $SPHK2^{+}$ monocyte-derived $CD11b^{+}$ macrophages, which are recruited to the airspace, in promoting anti-inflammatory function of alveolar macrophages during lung injury. They showed that S1P generated by recruited $SPHK2^{+}$ monocyte-derived $CD11b^{+}$ macrophages suppressed STING signaling in alveolar macrophages to resolve inflammatory injury [21]. Furthermore, Huang et al. investigated the role of mitochondria in vascular endothelial injury during sepsis and demonstrated that pore-forming molecule Gasdermin D released mitochondrial DNA into the cytosol, which set into motion an amplified response resulting in suppression of endothelial regeneration mediated by the cytosolic DNA sensor cGAS [22]. However, whether vascular endothelial cells-immune cells interactions are responsible for STING-mediated pulmonary inflammation during ALI, therefore, remains to be explored.

In this study, we demonstrated that inhibition of STING by C-176 intervention greatly repressed pulmonary inflammation responses in the LPS-induced murine model of acute lung injury. Moreover, we unveiled that STING inhibitor or STING knockdown regulated vascular endothelial cells-mediated immune cells adhesion and migration process via inhibiting the phosphorylation of signal transducer and activator of transcription 1 (STAT1). This may open up new opportunities for ALI treatment through STING inhibitor via modulating the vascular endothelial cells-immune cells crosstalk.

MATERIALS AND METHODS

Cell culture and treatment

HMEC-1 cells, HL-60 cells, and THP-1 cells were purchased from American Type Culture Collection (ATCC, Manassas, VA, USA). HMEC-1 cells were maintained in MCDB131 medium, HL-60 cells and THP-1 cells were maintained in RPMI-1640 medium (Gibco, Grand Island, NY, USA), containing 10% fetal bovine serum (HyClone, Logan, UT, USA), 100 U/mL penicillin, and 100 μg/mL streptomycin. Cells were cultured in a humidified incubator with 5% CO_2 at 37 °C. To be differentiated, HL-60 cells were cultured in a medium containing 1.25% DMSO (Sigma-Aldrich, St. Louis, MO, USA) and 10% FBS for 6 days.

In vitro leukocytes adhesion

HMEC-1 cells were treated with human STING inhibitor H-151 (HY-112693, CAS No.: 941987-60-6) (MedChemExpress, New Jersey, USA) [23] for 1 h and then stimulated with TNF-α (315-01A-50, Peprotech, London, UK) for 24 h. THP-1 monocytes and differentiated HL-60 cells were fluorescently labeled with Calcein AM (564061, Abcam Ltd) in RPMI-1640 medium for 30 min. Washing twice with PBS, THP-1 cells and differentiated HL-60 cells were added onto an HMEC-1 monolayer and incubated for 30 min, respectively. The cells were washed with PBS three times to remove non-adherent cells and were fixed with 3.7% formaldehyde for 15 min. The cells were visualized and imaged by fluorescence microscope (Olympus IX73, Tokyo, Japan) and were counted in three microscopic fields of each well. The pictures were analyzed by using ImageJ software.

Chemotaxis assay

HMEC-1 cells were treated with H-151 for 1 h and then stimulated with TNF-α for 24 h. Subsequently, conditional medium was collected and added into the lower chamber of 24-well trans-well chambers with 8 μm pores (Corning, NY, USA). THP-1 and differentiated HL-60 cells were labeled with Calcein AM (564061, Abcam Ltd) in RPMI-1640 medium for 30 min. After washing twice with PBS, THP-1 and differentiated HL-60 cells were resuspended in fresh RPMI-1640 medium and then added onto upper chamber of trans-well for 2 h incubated at 37 °C. The number of cells in the lower chamber was detected by cell counter and fluorescence microscope (Olympus IX73, Tokyo, Japan) [24].

SiRNA transfection

To knock down the STING expression in HMEC-1 cells, siRNA targeting for STING silence (RiboBio, Guangzhou, China) was used following the manufacturer's instructions. Briefly, cells were transiently transfected with appropriate siRNA using Lipofectamine® RNAiMAX Reagent (Thermo Fisher Scientific) in serum-free Opti-MEM medium. Cells were collected and assayed for STING expression 48 h later. SiRNA oligo sequences were listed in Supplementary Table S4.

In vivo animal experiments

All animals' feeding and laboratory programs were implemented according to the National Institutes of Health Guide for Care and Use of Laboratory Animals and approved by the Bioethics Committee of the Shanghai Institute of Materia Medica, Chinese Academy of Sciences. Male C57BL/6J mice (8 weeks, 20–22 g) were obtained from Shanghai Jihui Laboratory Animal Care Co. Ltd. (Certificate No. 2013-0018, China). The mice were maintained under specific pathogen-free conditions with a period of 12 h of light/12 h of darkness, suitable temperature, and humidity.

LPS-induced acute lung injury was induced as described by de Souza Xavier Costa et al. [25]. Briefly, mice were kept in an acrylic chamber (29 cm × 24 cm × 16 cm) throughout the LPS exposure period. A solution containing 0.5 mg/mL LPS (L2880, Sigma-Aldrich, MO, USA) in saline was aerosolized with an ultrasonic nebulizer (Sansbio, Nanjing, China) and air pump coupled to a manometer (flow rate was monitored and adjusted to 1 mL/min) for 30 min. After atomization for 30 min, the interval was 2 h, then atomized for 30 min again, and the experiment endpoint was in 4 h. Mice were randomly divided into four groups with eight mice per group: untreated normal control, vehicle challenged with LPS, LPS + C-176 (15 mg/kg), and LPS + C-176 (30 mg/kg). C-176 (HY-112906, CAS No.: 314054-00-7) was purchased from MedChemExpress (New Jersey, USA) and was dissolved in 200 μL of corn oil (Sigma-Aldrich, MO, USA) with a final concentration at 15 mg/kg and 30 mg/kg, was injected intraperitoneally 30 min before LPS inhalation.

Bronchoalveolar lavage fluid (BALF) collection

For the BALF collection, a tracheostomy was performed and a cannula was inserted into trachea. The left lung was lavaged three times with 1 mL cold PBS via tracheal catheter to obtain bronchoalveolar lavage (BAL) fluid. Counted the total number of cells in BALF. BALF was centrifuged at 4 °C at 600 × *g* for 10 min.

The differential cells were analyzed with flow cytometer using BD LSRFortessa instruments. The supernatant was stored at −20 °C until further examination.

Histology analysis

After mice were sacrificed, lung tissues were excised. The lung tissues were fixed in 4% paraformaldehyde at room temperature and then embedded in paraffin. Sections (5 μm) were cut, hematoxylin and eosin (H&E) staining were performed according to standard protocol. Histopathological evaluation was observed by two independent investigators blinded to the experimental conditions, in the Center for Drug Safety Evaluation and Research, Shanghai Institute of Materia Medica, Chinese Academy of Sciences, which is compliant with Good Laboratory Practice. Lung injury was scored according to the following criteria [26]: (1) alveolar congestion, (2) hemorrhage, (3) infiltration or aggregation of neutrophils in airspace or vessel wall, and (4) thickness of the alveolar wall. For each subject, a five-point scale was applied: 0, minimal (little) damage; 1+, mild damage; 2+, moderate damage; 3+, severe damage; and 4+, maximal damage. Points were added up and are expressed as median ± range of injury score.

For immunohistochemistry, tissue sections were blocked with 10% normal horse serum and incubated overnight at 4 °C in a humidified environment with F4/80 mAb (Abcam Ltd) and Ly6G mAb (Abcam Ltd). Primary labeling was detected using biotinylated horse anti-rabbit IgG secondary antibody, followed by color development with the aminoethyl carbazole system. All images were captured using a Leica TCS SPS microscope.

Cytokine analysis

Cytokines in BALF, lung homogenates, and cell supernatants were determined by ELISA kit. Lung tissues from mice were homogenized in PBS and centrifuged. The concentration of total protein was determined by BCA protein assay kit. Cytokine levels of TNF-α, IL-1β, IL-6, IL-12 were quantified by ELISA kit (BD Pharmingen) according to the manufacturer's instructions. The cytokine levels in the lung homogenates were expressed as pg/mg protein. And the cell supernatants and BALF were expressed as pg/mL.

Flow cytometry analysis

To obtain lung single-cell suspensions, the lung tissues were cut into small pieces in digestion buffer containing 1.5 mg/mL collagenase IV (C5138, Sigma-Aldrich, St. Louis, MO, USA) and 0.04 mg/mL DNase I (10104159001, Roche, Mannheim, Germany) for 1 h at 37 °C. Then the lung tissues were filtered with 100 μm strainer and red blood cells were depleted with erythrocyte lysate. Total lung cell suspensions were collected by centrifugation at 1200 r/min for 5 min and filtered by 70-μm strainer. The lung single-cell suspension was blocked with anti-mCD16/CD32 (2.4G2) and then stained with indicated antibodies. Flow cytometric analysis was performed on BD LSRFortessa, and data were analyzed using FlowJo 10 software (Treestar, Ashland, OR, USA). Immune cells were identified as $CD45^+$ (565967, BD Pharmingen), macrophages as $CD11b^+F4/80^+$ (550993 and 565410, BD Pharmingen), neutrophils as $CD11b^+Ly6G^+$ (551461, BD Pharmingen).

Measurement of double-stranded DNA

Double-stranded DNA was measured in BALF using Quant-iT™ PicoGreen™ dsDNA Reagent (P7581, ThermoFisher Scientific, Waltham, USA) according to the manufacturer's protocol.

Assessment of myeloperoxidase (MPO) activity

For measured neutrophil infiltration into lung tissues, MPO activity was detected by O-dianisidine method as previously described [27]. The results were shown as activity units per milligram tissue.

Real-time quantitative polymerase chain reaction (RT-QPCR) analysis

Total RNAs from lung tissues and culture cells were isolated using TRIzol reagent (Invitrogen, Carlsbad, CA, USA). Reverse transcription was carried out with Trans-Script First-Strand cDNA Synthesis SuperMix Kit (11123ES60, Yishen, Shanghai, China) according to the manufacturer's instructions. Subsequently, the product from reverse transcription was amplified with SYBR Green (11203ES08, Yishen, Shanghai, China) using Applied Biosystems (ThermoFisher Scientific, Waltham, USA). Primer sequences were listed in Supplementary Table S1.

Western blot analysis

Lung tissue samples and culture cells were lysed in SDS lysis buffer (P0013G, Beyotime, Shanghai, China). Electrophoresis was performed as we have described previously [28]. Western blots were quantified using ImageJ software. Antibody information was listed in Supplementary Table S3.

Chromatin immunoprecipitation (ChIP) assay

HMEC-1 cells were well stimulated with TNF-α for 24 h following pretreatment with H-151 for 1 h. And cells were collected for ChIP assay according to a previously described protocol [29]. Vcam-1- and Ccl2-specific primers were designed to include the STAT1–binding site. The primer sequences are listed in Supplementary Table S2.

Statistical analysis

All experiment data were presented as mean ± SEM and statistically evaluated by one-way ANOVA followed by Dunnett's test for three or more groups. Statistical analyses were evaluated using GraphPad Prism 7.0 software. Differences where $P < 0.05$ were considered statistically significant.

RESULTS

The cGAS-STING pathway was upregulated in the LPS-induced ALI mice model and STING inhibitor downregulated its activation

Endotoxin-induced ALI is a well-characterized model of nonlethal ALI mediated by pro-inflammatory activation of immune cells and increased vascular permeability [30]. In our study, we investigated the potential role of STING on the progression of lung inflammation using the LPS-induced ALI model (Fig. 1a). Mice were randomly divided into four groups with eight mice per group: untreated normal control, vehicle challenged with LPS, LPS + C-176 (15 mg/kg), and LPS + C-176 (30 mg/kg). STING inhibitor was injected intraperitoneally 30 min before model every atomizing. Western blot analysis showed that cGAS and STING were significantly increased in the vehicle group lung tissues homogenates (Fig. 1c). Accordingly, the phosphorylation levels of TBK1 and p65, which are the direct downstream signaling proteins of STING, were significantly increased in LPS-challenged vehicle group mice (Fig. 1d). Compared with the vehicle group, selective antagonist C-176 treatment decreased the levels of STING (Fig. 1b and c) and inhibited the phosphorylation of TBK1 and p65 (Fig. 1d), consistent with Haag's findings [23]. Additionally, STAT1 phosphorylation was significantly increased in LPS-challenged vehicle group mice and C-176 treatment inhibited the phosphorylation of STAT1 (Fig. 1d), followed by a decrease of the downstream interferon-stimulated genes (ISGs) including *Isg15*, *Mx-1*, *Isg56*, and *Eif2ak2* (Fig. 1e). These results indicated that cGAS-STING pathway participates in the development of LPS-mediated ALI.

Suppression of STING ameliorated lung inflammation in ALI mice

The above findings encouraged us to further investigate the important role of STING in lung injury. Compared with the vehicle group, H&E-stained pulmonary sections indicated that

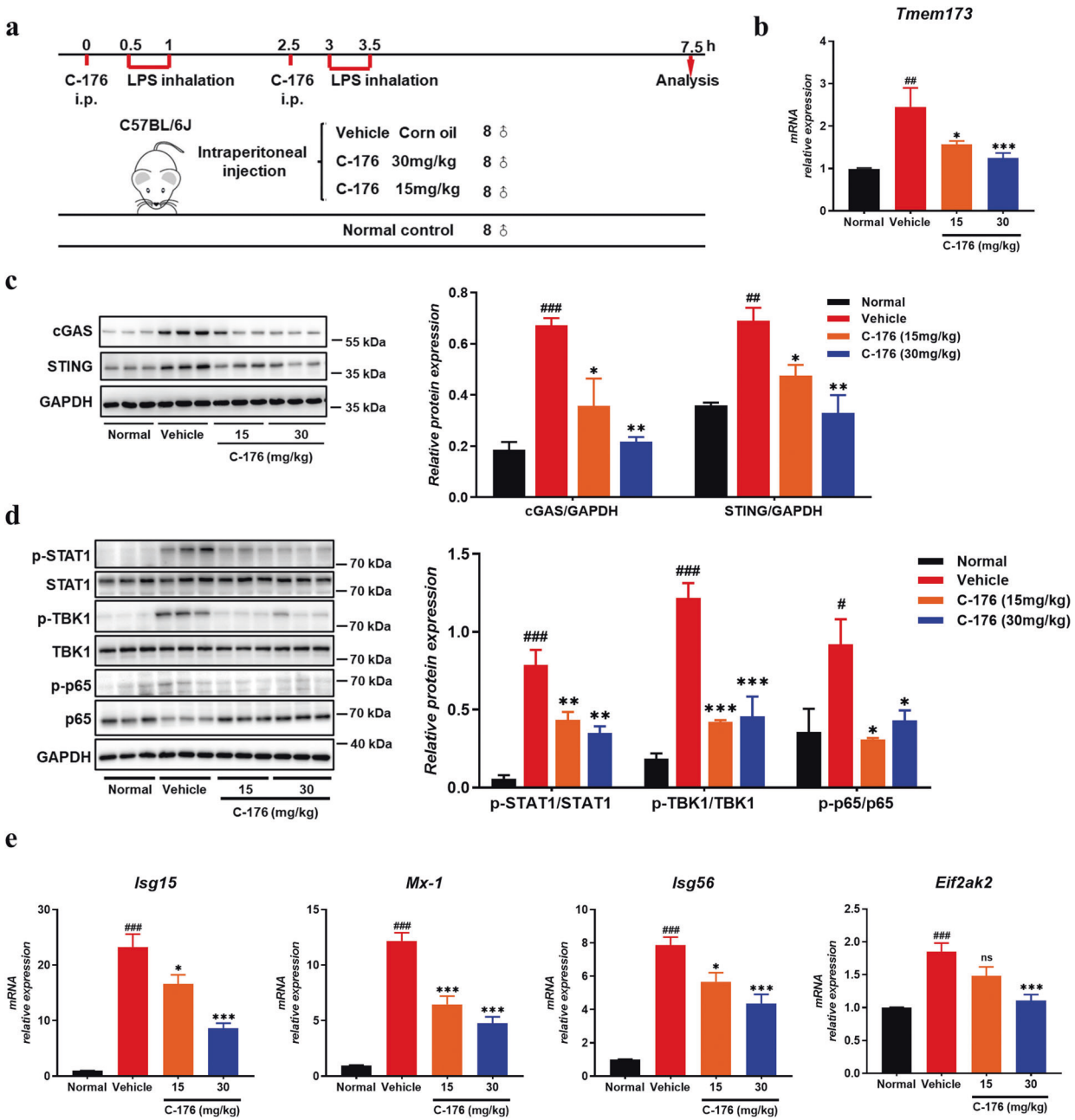

Fig. 1 The cGAS-STING signaling was involved in LPS-induced ALI. a The flow diagram of LPS-induced ALI mice model. **b** *Sting* mRNA level was determined in lung tissues homogenates ($n = 8$ mice per group). **c** cGAS and STING protein levels were detected in lung tissues homogenates by Western blot ($n = 3$ mice per group). The value of relative protein expression represented the ratio of targeted protein quantitative value to GAPDH quantitative value in each lane. **d** Western blot analysis of downstream protein phosphorylation (TBK1, p65, and STAT1) in lung tissues homogenates and GAPDH was used as a loading control ($n = 3$ mice per group). The value of relative protein expression represented the ratio of phosphorylated protein quantitative value to total protein quantitative value in each lane. **e** RT-QPCR analysis of ISG factors including *Mx-1*, *Isg15*, *Isg56*, and *Eif2ak2* mRNA extracted from lung tissues ($n = 8$ mice per group). Data are presented as means ± SEM. Normal: untreated control, Vehicle: mice challenged with LPS. Western blots were quantified using ImageJ software. The mRNA relative levels were normalized to normal group mice by the $2^{-\triangle\triangle Ct}$ method. $^{*}P < 0.05$, $^{**}P < 0.01$, $^{***}P < 0.001$ compared to vehicle group. $^{\#}P < 0.05$, $^{\#\#}P < 0.01$, $^{\#\#\#}P < 0.001$ compared to normal group.

alveolar architecture damage and congestion were relieved in STING inhibitor-treated groups (Fig. 2a), along with a decrease in the levels of BALF protein (Fig. 2b). Meanwhile, STING inhibition also reduced the levels of dsDNA in BALF (Fig. 2c) and attenuated lactate dehydrogenase activity (Fig. 2d) in serum. In addition, massive infiltration of immune cells and subsequent inflammatory cytokines production can further aggravate the development of the disease [31]. The histological result revealed that the number of infiltrating cells was reduced when C-176 treatment was applied (Fig. 2a), accompanied by less accumulation of BALF cells (Fig. 2e). As shown in Fig. 2f, C-176 treatment significantly lessened the production of pro-inflammatory cytokines including TNF-α, IL-6, IL-12, and IL-1β in BALF. Consistently, the protein and gene levels of pro-inflammatory

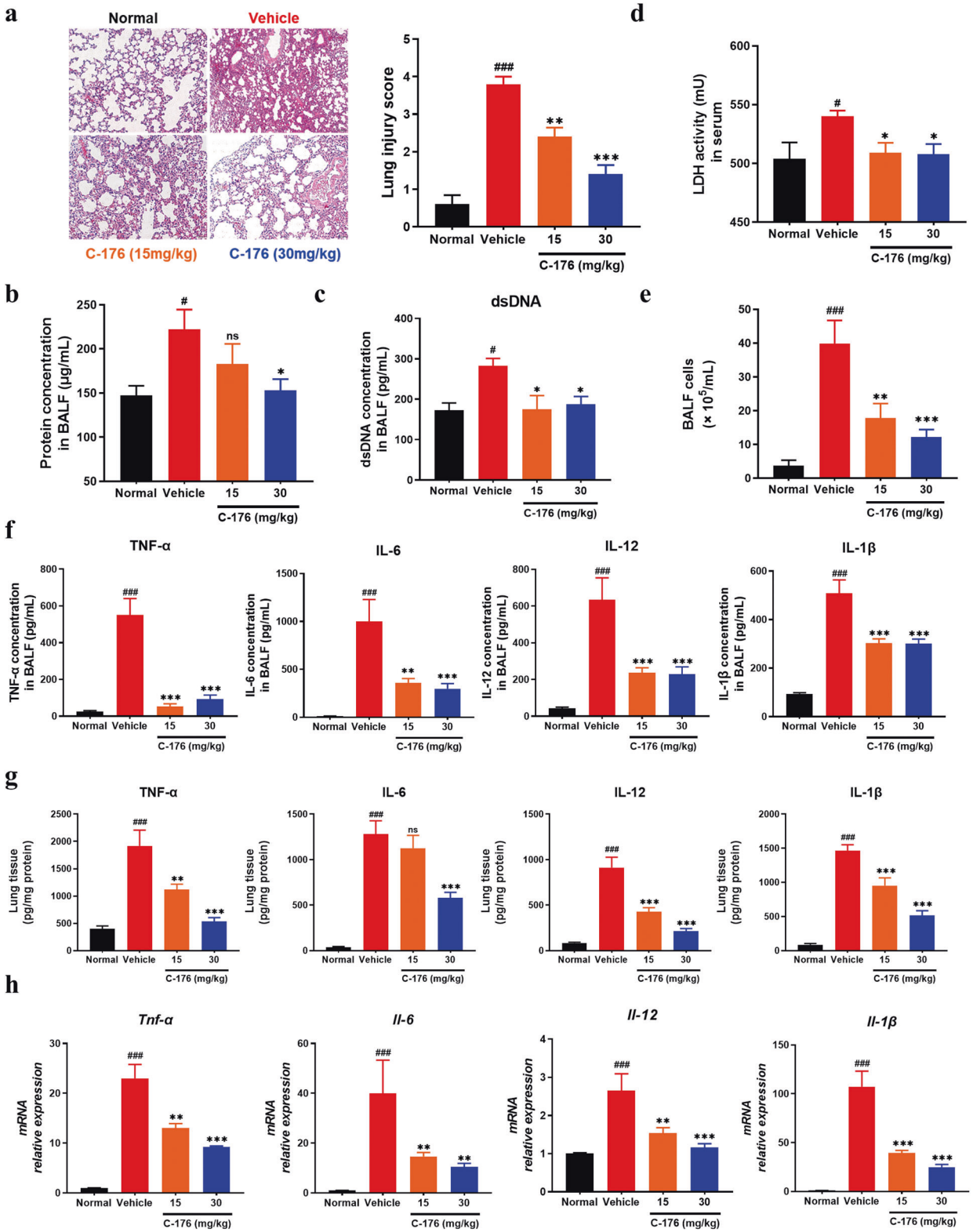

Fig. 2 Inhibition of STING attenuated lung inflammation in the LPS-induced ALI mice. a Representative microscopic pictures of the H&E-stained lung tissues section were shown. Scale bars, 50 μm. **b** The protein content in BALF was measured. **c** The concentration of dsDNA release was detected in BALF. **d** The production of LDH in serum was detected. The total number of cells (**e**) and proinflammatory cytokines (**f**) in BALF were measured. **g** The levels of cytokines (TNF-α, IL-6, IL-12, and IL-1β) in lung tissues homogenates were measured by ELISA. **h** Pro-inflammatory cytokines mRNA levels were determined in lung tissues homogenates. Data are presented as means ± SEM. Normal: untreated control, Vehicle: mice challenged with LPS. $n = 8$ mice per group. The mRNA relative levels were normalized to normal group mice by the $2^{-\triangle\triangle Ct}$ method. $^{*}P < 0.05$, $^{**}P < 0.01$, $^{***}P < 0.001$ compared to vehicle group. $^{\#}P < 0.05$, $^{\#\#\#}P < 0.001$ compared to normal group.

cytokines in the lung homogenates were decreased in C-176 treated animals (Fig. 2g, h). Taken all together, suppression of the STING decreased the severity of ALI and lowered the LPS-mediated inflammation.

STING inhibitor restrained the infiltration of neutrophils in the LPS-induced ALI mice model

The above data suggested that STING inhibitor affected the infiltration of immune cells into the lung tissues of mice. We performed an immunohistochemical assay to further investigate the types of infiltrating immune cells. Our data indicated that the infiltration of F4/80$^+$ macrophages (Supplementary Fig. S1a) and Ly6G$^+$ neutrophils significantly increased in the vehicle group, and STING inhibitor could relieve this symptom (Fig. 3a). Meanwhile, increased populations of macrophages (Supplementary Fig. S1b) and neutrophils (Fig. 3b) were observed in BALF from LPS-induced mice, which could be restored by C-176. In addition, flow cytometric analyses showed that treatment with STING inhibitor substantially reduced the percentage of CD11b$^+$Ly6G$^+$ neutrophils in lung tissues, compared with vehicle control mice (Fig. 3c). Myeloperoxidase (MPO), which is most abundantly expressed in neutrophil granulocytes, showed enhanced activity in lung tissues of ALI mice and C-176 inhibited MPO activity, indicating the decrease of neutrophil infiltration (Fig. 3d). Correspondingly, the gene expression of Ly6G and neutrophil extracellular traps (NET) markers (Pad4 and Rac2) in lung tissues was downregulated by C-176 (Fig. 3e). Besides, infiltrating macrophages may aggravate the development of pulmonary inflammation through the activation of the inflammasome. Our results revealed that *Asc* and *Caspase-1* were highly induced in the lung of vehicle-treated LPS animals, whereas C-176 treatment inhibited the induction of these genes by QPCR assay (Supplementary Fig. S1d). We also observed that administration of C-176 dampened the expression of inflammasome components including NLRP3 and caspase-1 in lung homogenates (Supplementary Fig. S1c), consistent with Geng's data [20]. Vascular endothelial cells play a key role in recruiting circulating immunocytes by secreting chemokines and guiding immunocytes' transmission by expressing adhesion molecules, thus leading to the maintenance and aggravation of inflammation in ALI. To further clarify the mechanism by which STING inhibitor affected the infiltration of macrophages and neutrophils into the lungs of mice, we examined the chemokines and adhesion molecules expressed [32]. Gene expression assays showed that the levels of chemokines and chemokine receptors (such as *Cxcl10*, *Cxcl2*, *Cxcl9*, *Cxcl1*, *Ccl2*, *Ccl20*, *Ccl3*, *Ccl4*, *Ccl5*, *Ccl22*, and *Ccr2*) were significantly enhanced in LPS-induced vehicle group mice, while C-176 treatment inhibited the expression (Fig. 3f). As shown in Fig. 3g, h, the adhesive molecule VCAM-1 was significantly enhanced in vehicle mice, while C-176 treatment restored the expression almost to the normal level. These results suggested that STING inhibitor repressed the infiltration of macrophages and neutrophils and reduced pulmonary inflammation.

Inhibition of STING suppressed the expression of chemokines and adhesive molecules in vascular endothelial cells

Following the decreased adhesive molecule level after STING inhibition in vivo, we used TNF-α-stimulated HMEC-1 (common and classic vascular endothelial cells) to study the effects of human STING inhibitor H-151 [23] on the adhesive and migrating process in vitro. CCK-8 assay shows that H-151 at 90 μM and below had almost no toxicity to HMEC-1 cells (Supplementary Fig. S2). TNF-α addition increased the expression of chemokines including *Ccl2*, *Ccl5*, *Ccl20*, and *Cxcl10*, while H-151 possessed the capacity to downregulate the expression of chemokines in a dose-dependent manner (Fig. 4a). Moreover, STING inhibitor could decrease adhesive molecule VCAM-1 expression from HMEC-1 cells (Fig. 4b, c). To further verify the effect of STING inhibition on the functional profile of HMEC-1 cells, we knocked down the expression of STING in HMEC-1 cells and analyzed the effects of STING on chemokines and adhesive molecules. The interference efficiency of STING siRNAs was above 90% (Supplementary Fig. S3a, b). Consistent with the STING inhibitor, knockdown of STING also inhibited the expression of chemokines (including *Ccl2*, *Ccl5*, *Ccl20*, and *Cxcl10*) and adhesive molecule VCAM-1 in TNF-α-stimulated HMEC-1 (Fig. 4d, e, and f).

Finally, we used HMEC-1 cells to explore their adhesive ability and chemotaxis effects on monocytes and neutrophils. As shown in Fig. 4g and Supplementary Fig. S4 (upper), enhanced the adhesive ability of HMEC-1 toward differentiated HL-60 cells and THP-1 was observed under the stimulation of TNF-α and STING inhibition intervened in this event. In accordance with the decreased chemokines level after STING inhibition, the chemotaxis behavior of THP-1 (Supplementary Fig. S4, below) and differentiated HL-60 cells (Fig. 4g, below) to conditional media from HMEC-1 cells was restrained by STING inhibition. These results suggested that STING may participate in the interaction between vascular EC and immunocytes, and then restrained the infiltration of macrophages and neutrophils, which possibly becomes one of the underlying mechanisms of STING mediating lung inflammation.

STING inhibitor suppressed the expression of Ccl2 and VCAM-1 via inhibiting the phosphorylation of STAT1

To ravel the underlying molecule mechanism of how STING inhibitor affected the expression of chemokines and VCAM-1 from vascular endothelial cells, we first analyzed the classical downstream pathways of TNF-α stimulation like p65 and mitogen-activated protein kinases (MAPK) signaling. The phosphorylation of p65 and MAPK increased after TNF-α treatment, while H-151 treatment could not reduce the upregulation of protein phosphorylation (Fig. 5a). Meanwhile, immunofluorescence staining showed that p65 nuclear translocation could not be influenced with H-151 treatment (Supplementary Fig. S5). Surprisingly, H-151 and STING knockdown highly suppressed the phosphorylation of STAT1, which is a transcription factor strongly associated with the activation of STING (Fig. 5b, c). We then investigated the exact role of STAT1 in endothelial cells. We found that the 5′ untranslated region of the *Ccl2* and *Vcam-1* gene contains putative STAT1 binding sites via analyzing with TFSEARCH (Searching Transcription Factor Binding Sites, version 1.3) (Fig. 5d). Results from ChIP assay showed that STAT1 bound to the *Ccl2* and *Vcam-1* promoter, this binding was strikingly decreased by H-151 treatment compared with control cells (Fig. 5e). Similarly, silencing STING prevented the binding between STAT1 and the *Ccl2* and *Vcam-1* promoter (Fig. 5f), confirming the role of STING in promoting this binding and *Ccl2* and *Vcam-1* expression. These results suggested that STING inhibition suppressed the expression of Ccl2 and VCAM-1 via inhibiting STAT1 consensus sites to genes promoter upstream.

DISCUSSION

Increasing evidence has been reported on the regulatory role of cGAS-STING signaling pathway in various inflammatory diseases including acute pancreatitis, alcoholic liver disease, age-dependent macular degeneration, acute kidney injury (AKI), and nonalcoholic steatohepatitis [33–37]. In this study, we disclose a critical role of STING in LPS-induced ALI which modulates vascular endothelial cells–mediated immune cells chemotaxis and adhesion via regulating phosphorylation of STAT1 (Fig. 6).

Actually, targeting STING by inhibitor C-176 has been shown to be effective in the treatment of inflammatory diseases. Similar to our results (Fig. 1d), Hagg's work showed that C-176 could inhibit the phosphorylation of TBK1, reduce the CMA-mediated induction of serum levels of type I IFN and IL-6, improve signs of severe multi-organ inflammation in Trex1$^{-/-}$ mice, which accompanied by persistent activation of the cGAS-STING pathway and certain pathogenic features of Aicardi–Goutières syndrome in humans

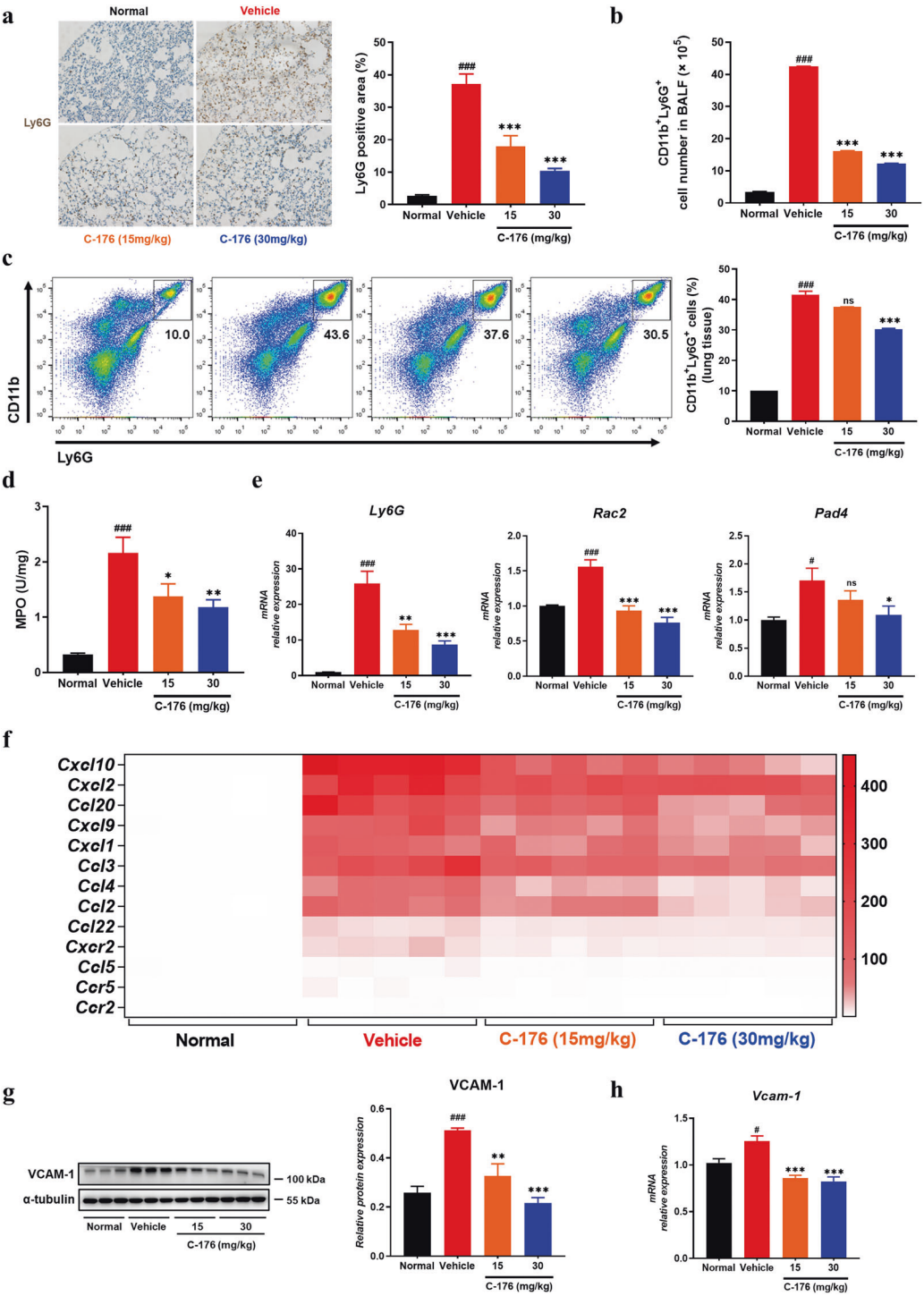

Fig. 3 STING inhibitor restrained the infiltration of neutrophils and influenced the expression of chemokines and adhesive molecules. **a** Immunohistochemical staining for Ly6G of lung tissue. Scale bars, 100 μm. **b** The cell number of $CD11b^{+}Ly6G^{+}$ neutrophils in BALF by FACS. **c** The population of $CD11b^{+}Ly6G^{+}$ neutrophils in lung tissues. **d** MPO activity in the lung tissues. **e** The mRNA expression of Ly6G, Rac2, and Pad4 in lung tissues homogenates. **f** Gene expression levels of various chemokines and chemokines receptors in lung tissues homogenates by RT-QPCR. The expression levels of VCAM-1 were determined by Western blot analysis (**g**) ($n = 6$ mice per group) and RT-QPCR (**h**) in lung tissues. The value of relative protein expression represented the ratio of targeted protein quantitative value to α-tubulin quantitative value in each lane. Data are presented as means ± SEM. Normal: untreated control, Vehicle: mice challenged with LPS. $n = 8$ mice per group. The mRNA relative levels were normalized to normal group mice by the $2^{-\triangle\triangle Ct}$ method. $^{*}P < 0.05$, $^{**}P < 0.01$, $^{***}P < 0.001$ compared to vehicle group. $^{\#}P < 0.05$, $^{\#\#\#}P < 0.001$ compared to normal group.

[23]. Peng's data demonstrated that administration of C-176 substantially attenuated subarachnoid hemorrhage-induced brain edema and neuronal inflammation and improved neurological function by activating AMP-activated protein kinase signal [38]. In addition, Maekawa et al. found that pharmacological inhibition of the STING by C-176 attenuated tubular injury and renal function in association with a reduction of tubular inflammation in cisplatin-induced AKI mice [39].

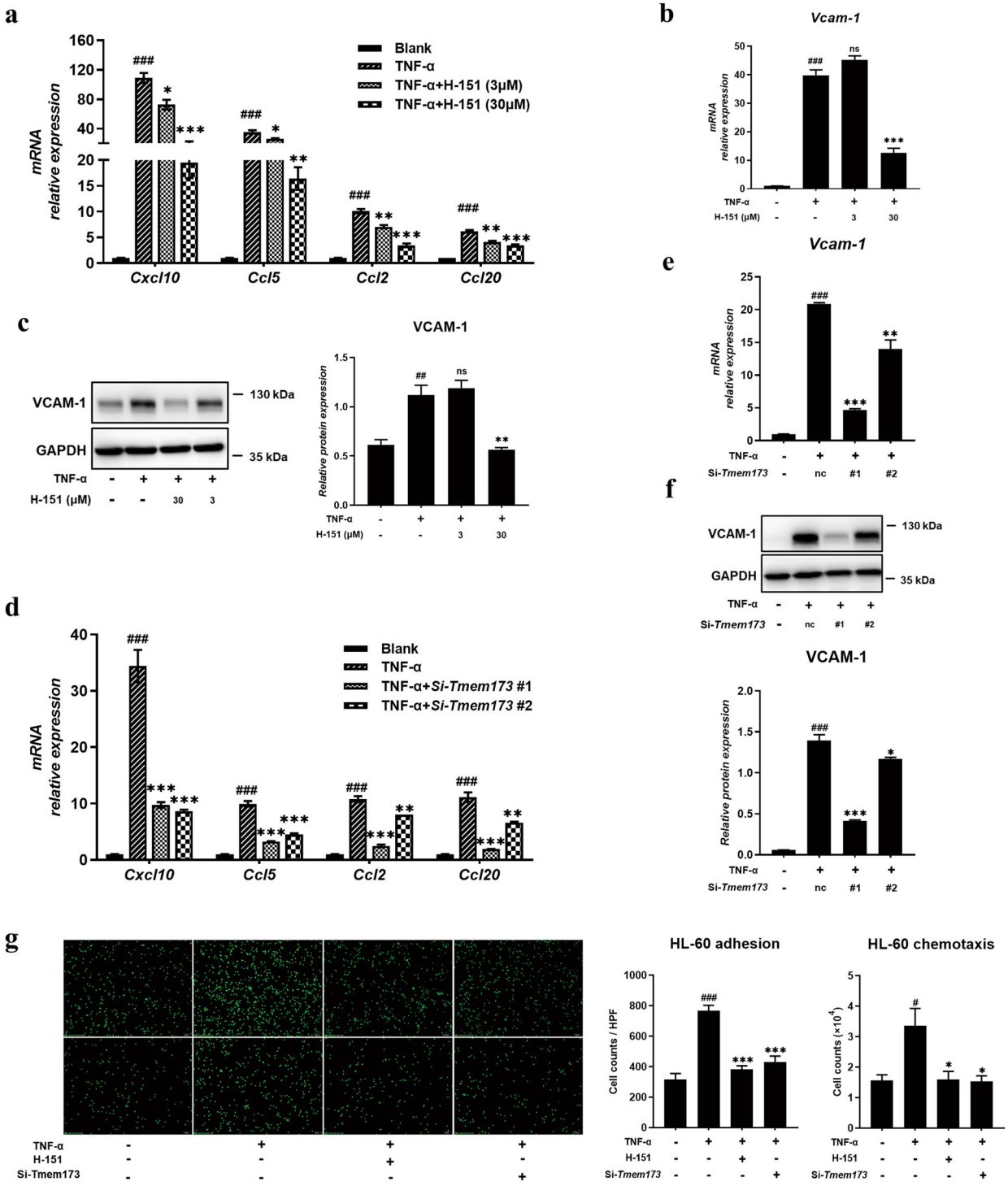

Fig. 4 Inhibition of STING suppressed the expression of chemokines and adhesive molecules in vascular endothelial cells. HMEC-1 cells were seeded into 12-well plates at a density of ~2×10^5/well, then pre-treated with the indicated concentration of H-151 for 1 h and subsequently cells were stimulated with TNF-α for 24 h. **a** RT-QPCR analysis of chemokines on RNA extracted from HMEC-1 cells was measured. The expression of VCAM-1 in HMEC-1 cells at different inhibitor concentrations upon TNF-α stimulation by RT-QPCR (**b**) and Western blot (**c**). HMEC-1 cells were transfected with STING siRNA or NC siRNA for 48 h and subsequently, cells were stimulated with TNF-α for 24 h. **d** RT-QPCR analysis of chemokines on RNA extracted from HMEC-1 cells was measured. The expression of VCAM-1 in HMEC-1 cells by RT-QPCR (**e**) and Western blot (**f**). **g** Representative images of differentiated HL-60 cells adhesion to the HMEC-1 cells were captured (upper panel). Representative images of differentiated HL-60 cells chemotaxis to the HMEC-1 cells were captured (below panel). Scale bars, 100 μm. Data are presented as means ± SEM of three independent experiments. $^{*}P < 0.05$, $^{**}P < 0.01$, $^{***}P < 0.001$ compared to TNF-α stimulation. $^{\#}P < 0.05$, $^{\#\#}P < 0.01$, $^{\#\#\#}P < 0.001$ compared to no stimulation. Nc means control scrambled siRNA.

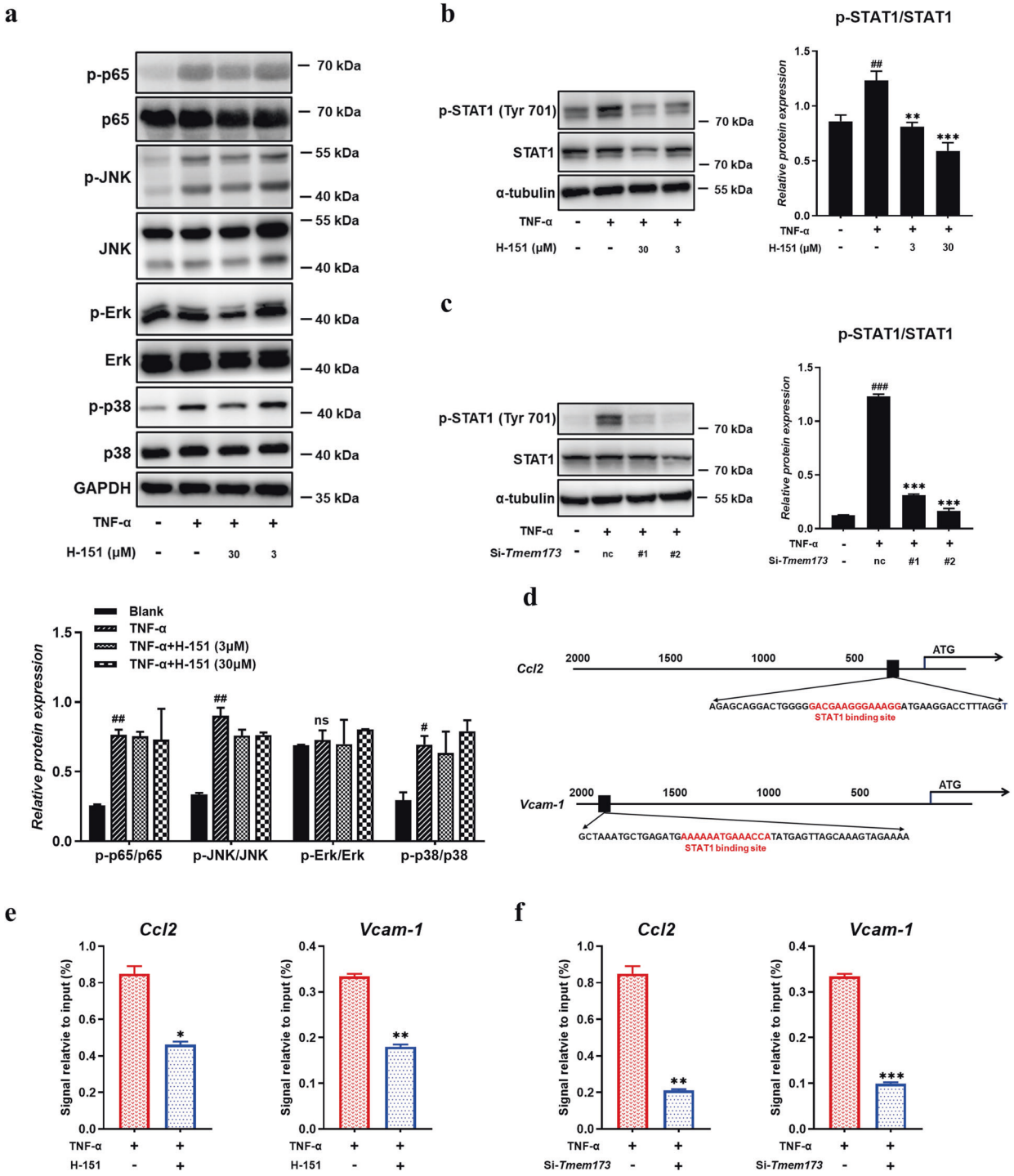

Fig. 5 STING inhibitor suppressed the expression of chemokine Ccl2 and adhesive molecule Vcam-1 via inhibiting the phosphorylation of STAT1. a P65 and MAPK signaling pathways were detected in TNF-α stimulated HMEC-1 cells. **b**, **c** Western blot analysis of p-STAT1 in TNF-α stimulated HMEC-1 cells. **d** A putative STAT1 binding site upstream of the 5′UTR of *Vcam-1* and *Ccl2* was shown. **e**, **f** Chromatin immunoprecipitation assay for the *Vcam-1* and *Ccl2* promoter was performed with anti-STAT1 antibody. Data are presented as means ± SEM of three independent experiments. $^{*}P < 0.05$, $^{**}P < 0.01$, $^{***}P < 0.001$ compared to TNF-α stimulation. $^{\#}P < 0.05$, $^{\#\#}P < 0.01$, $^{\#\#\#}P < 0.001$ compared to no stimulation. Nc means control scrambled siRNA.

In fact, the role of STING in experimental ALI has also been mentioned in a few studies recently. Both Geng's and Mehta's groups reported that STING knockout regulates the function of macrophages and ameliorates LPS-induced murine ALI. Geng's data found that mt-DNA in cytosol activated and upregulated STING, which subsequently led to NLRP3 inflammasome activation and pyroptosis of macrophages [20]. Consistent with these observations, our data also showed that inflammasome components were highly increased in the lung of vehicle-treated LPS animals by realtime PCR and immunoblots assay, whereas STING inhibitor C-176 intervention inhibited the activation of inflammasome (Supplementary Fig. S1c, d). Besides, Mehta's study

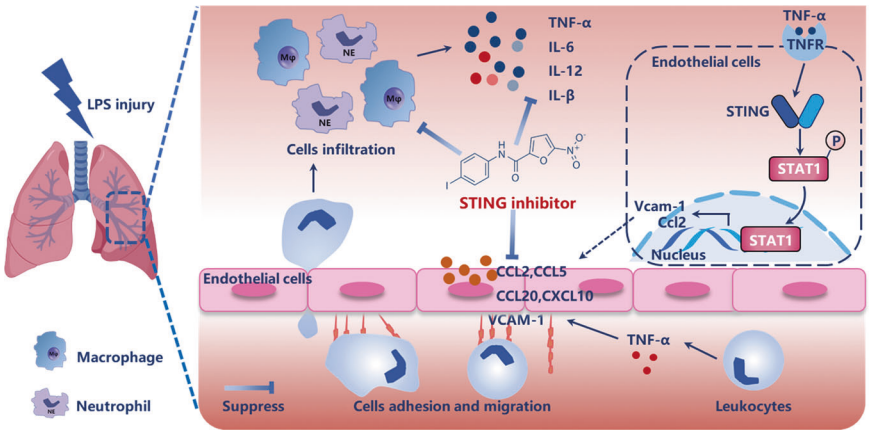

Fig. 6 Diagram of how STING inhibitor alleviated endotoxin-induced acute lung injury. LPS inhalation leads to the activation of vascular endothelial cells. Once activated, vascular endothelial cells secrete the chemokines (such as *Ccl2*, *Ccl5*, *Ccl20*, and *Cxcl10*) and recruit neutrophils and macrophages, resulting in the massive production of inflammatory cytokines and further inflammatory positive feedback loop. STING inhibitor attenuates vascular endothelium activation, prevents vascular endothelial cells–mediated immune cells chemotaxis and adhesion, and inhibits the macrophages and neutrophils infiltration, and relieves inflammation. Mechanistically, STING inhibition downregulates the phosphorylation of transcription factor STAT1, which subsequently influences the binding of chemokine and adhesive molecule gene promoter.

demonstrated that the cell-intrinsic SPHK2-S1P pathway in airspace $CD11b^+$ macrophages blocked STING signaling in alveolar macrophages, thereby resolving lung vascular inflammatory injury [21]. They showed that depletion of $CD11b^+$ macrophages led to alveolar macrophage proliferation, neutrophil accumulation, and long-lasting vascular injury. In our study, we also found that STING inhibitor inhibited the infiltration of $CD11b^+F4/80^+$ macrophages (Supplementary Fig. S1a) in the lung lesion, thereby preventing lung inflammatory response.

Neutrophils are considered to play a key role in the progression of ALI, as activation and migration of neutrophils are early steps in the pulmonary inflammatory process. In experimental models, the elimination of neutrophils markedly decreases the severity of ALI. Furthermore, in neutropenic patients with lung injury, deterioration of pulmonary function as neutropenia resolves has been well described [40, 41]. In our study, we found that STING inhibitor could decrease the infiltration of $CD11b^+Ly6G^+$ neutrophils in lung tissues (Fig. 3a, c) and BALF (Fig. 3b) and inhibit MPO activity (Fig. 3d), which is most abundantly expressed in neutrophil granulocytes. Wei's group finds the release of mtDNA in acute peripheral tissue trauma models induced the formation of NETs and sterile inflammation. MtDNA activated neutrophils via cGAS-STING and TLR9 pathways and increased extracellular neutrophil-derived DNA in NETs and promoted the expression of the NET-associated proteins Rac 2 and Pad4 [42]. Correspondingly, our study showed that the gene expression of Pad4 and Rac2 in lung tissues was downregulated by STING inhibitor C-176 (Fig. 3e). Therefore, our findings suggested that STING inhibitor repressed the infiltration of neutrophils and reduced pulmonary inflammation.

Vascular endothelial cells are kind of sentinel cells detecting pathogen-associated molecular patterns or damage-associated molecular patterns in ALI, and activated vascular endothelial cells could mediate immune cell adhesion and chemotaxis [12, 43]. Increased vascular endothelial cells-immunocytes interaction facilitates immunocyte's transmigration from the capillaries into the lung parenchyma, contributing to the inflammatory response as well as to pulmonary edema formation. Therefore, understanding the molecular control of vascular endothelial cells activation is highly significant for elucidating the pathogenesis of ALI. Adhesion molecules play important roles in cell migration, proliferation, and signal transduction, as well as in development and tissue repair [44]. Here, we observed that STING inhibitor decreased vascular endothelial cells activation accompanied with VCAM-1 expression in vivo (Fig. 3g, h). Similarly, in vitro, there was a large increase of VCAM-1 expression during TNF-α stimulation in HMEC-1 cells, and STING inhibitor or STING siRNA showed steady inhibitory effects on the expression level (Fig. 4b, c, e, and f). In co-culture experiment, the adhesive ability of vascular endothelial cells towards neutrophils and macrophages was also restrained by human STING inhibitor and STING knockdown (Fig. 4g and Supplementary Fig. S4). It is worth noting that the expression of ICAM-1 failed to be relieved in LPS-induced lung injury or TNF-α triggered HMEC-1 cells under STING inhibitor intervention (data not shown). These data pointed out that STING may be specifically implicated in diseases mediated by vascular endothelium; whereas, the therapeutic effects of STING inhibitor on vascular diseases such as STING-associated vasculopathy with onset in infancy await further investigations.

Besides, chemokines released by endothelial cells are an initial pathological process for immune cells migration to the site of inflammation, and it could amplify the immune-inflammatory response in ALI [12]. *Ccl2*, *Ccl3*, *Ccl5*, and *Cxcl10*, involved in inflammatory and infection diseases, direct the migration and infiltration of monocytes, memory T lymphocytes at the place of injury and infection [45, 46]. In rodents, the most relevant chemokines for neutrophil recruitment into the lung are *Cxcl1* and *Cxcl2*, which bind to *Cxcr2* chemokine receptor. Inhibition or knockout of receptor *Cxcr2* diminishes neutrophil influx into the lung tissues [40]. Moreover, *Ccl3*, *Ccl5*, and *Ccl20* also act as chemotactic factors that attract lymphocytes and neutrophils [47]. Our data revealed that inhibition of STING reduced the expression of chemokines including *Ccl2*, *Ccl5*, *Ccl20*, and *Cxcl10* (Fig. 3f, Fig. 4a, d) and intervened in the migrating process of immunocytes towards HMEC-1 cells after TNF-α stimulation (Supplementary Fig. S4 and Fig. 4g). Collectively, this is the first study to disclose a regulatory role of STING on chemokine and adhesive molecule expression in vascular endothelial cells and further elucidate the mechanism of crosstalk between endothelial cells and immune cells, especially neutrophils.

The signaling pathway of activating endothelial cells by the mediator TNF-α derived principally from activated leukocytes has been extensively studied [11]. In brief, TNF-α binds to the TNF-α receptor and initiates various kinase cascades, leading to activation of the transcription factors p65 and activator protein 1. However, p65 phosphorylation and nuclear translocation increased after TNF-α stimulation in HMEC-1 cells and STING inhibitor treatment could not

reduce the upregulation of protein phosphorylation and nuclear translocation (Fig. 5a and Supplementary Fig. S5). In the present study, we demonstrated that the phosphorylation of STAT1 was upregulated in mice and HMEC-1 cells upon stimulation (Fig. 5b). STAT1 is a transcription factor strongly associated with the activation of STING. Studies have shown that the activation of STING could give rise to an increase of the phosphorylation of STAT1 in vascular and pulmonary syndrome and KRAS-driven lung cancers [48, 49]. Intriguingly, STING inhibitor or siRNA intervention both inhibited the increasing level of p-STAT1, further repressed the binding of STAT1 to the promoter of *Vcam-1* and *Ccl2* (Fig. 5e, f), indicating that STAT1 was involved in the transcription of genes associated with chemotaxis and adhesion process.

In summary, through the application of STING inhibitor, we explored a new function of STING involved in regulating the activation of vascular endothelial cells, and further clarified the role and mechanism of STING in the pathophysiological process in ALI. Altogether, the current study supports the notion that targeting STING might be a novel and promising therapeutic strategy against ALI.

ACKNOWLEDGEMENTS

This work was funded by the Science & Technology Commission of Shanghai Municipality, China (Grant No. 18431907100) and State Key Laboratory of Drug Research, Shanghai Institute of Materia Medica, Chinese Academy of Sciences (Grant No. SIMM2105KF-11).

AUTHOR CONTRIBUTIONS

BW, YWW, and WT designed project and contributed to the conception. BW, MMX, CF, CLF, QKL, HML, CGX, FB, and HYW performed research. BW and YWW analyzed data. BW, YWW, and WT wrote the paper. All authors contributed to the collection and interpretation of data and approved the final draft.

ADDITIONAL INFORMATION

Supplementary information The online version contains supplementary material available at https://doi.org/10.1038/s41401-021-00813-2.

Competing interests: The authors declare no competing interests.

REFERENCES

1. Mackay A, Al-Haddad M. Acute lung injury and acute respiratory distress syndrome. Contin Educ Anaesth Crit Care Pain. 2009;9:152–6.
2. Saguil A, Fargo MV. Acute respiratory distress syndrome: diagnosis and management. Am Fam Physician. 2020;101:730–8.
3. Rezoagli E, Fumagalli R, Bellani G. Definition and epidemiology of acute respiratory distress syndrome. Ann Transl Med. 2017;5:282.
4. He YQ, Zhou CC, Yu LY, Wang L, Deng JL, Tao YL, et al. Natural product-derived phytochemicals in managing acute lung injury by multiple mechanisms. Pharmacol Res. 2021;163:105224.
5. Cepkova M, Matthay MA. Pharmacotherapy of acute lung injury and the acute respiratory distress syndrome. J Intensive Care Med. 2006;21:119–43.
6. Villar J, Blanco J, Añón JM, Santos-Bouza A, Blanch L, Ambrós A, et al. The ALIEN study: incidence and outcome of acute respiratory distress syndrome in the era of lung protective ventilation. Intensive Care Med. 2011;37:1932–41.
7. Matthay MA, McAuley DF, Ware LB. Clinical trials in acute respiratory distress syndrome: challenges and opportunities. Lancet Respir Med. 2017;5:524–34.
8. Delano MJ, Ward PA. Sepsis-induced immune dysfunction: can immune therapies reduce mortality? J Clin Invest. 2016;126:23–31.
9. The Immunology of Cardiovascular Homeostasis and Pathology.
10. Wang L, Cao Y, Gorshkov B, Zhou Y, Yang Q, Xu J, et al. Ablation of endothelial Pfkfb3 protects mice from acute lung injury in LPS-induced endotoxemia. Pharmacol Res. 2019;146:104292.
11. Pober JS, Sessa WC. Evolving functions of endothelial cells in inflammation. Nat Rev Immunol. 2007;7:803–15.
12. Andonegui G, Goyert SM, Kubes P. Lipopolysaccharide-induced leukocyte-endothelial cell interactions: a role for CD14 versus toll-like receptor 4 within microvessels. J Immunol. 2002;169:2111–9.
13. Goldenberg NM, Steinberg BE, Slutsky AS, Lee WL. Broken barriers: a new take on sepsis pathogenesis. Sci Transl Med. 2011;3:88ps25.
14. Saeed AFUH, Ruan X, Guan H, Su J, Ouyang S. Regulation of cGAS-mediated immune responses and immunotherapy. Adv Sci. 2020;7:1902599.
15. Zhang X, Bai XC, Chen ZJ. Structures and mechanisms in the cGAS-STING innate immunity pathway. Immunity. 2020;53:43–53.
16. Hopfner KP, Hornung V. Molecular mechanisms and cellular functions of cGAS-STING signalling. Nat Rev Mol Cell Biol. 2020;21:501–21.
17. Hu MM, Shu HB. Innate immune response to cytoplasmic DNA: mechanisms and diseases. Annu Rev Immunol. 2020;38:79–98.
18. Motwani M, Pesiridis S, Fitzgerald KA. DNA sensing by the cGAS-STING pathway in health and disease. Nat Rev Genet. 2019;20:657–74.
19. Ablasser A, Chen ZJ. cGAS in action: expanding roles in immunity and inflammation. Science. 2019;363:eaat8657.
20. Ning L, Wei W, Wenyang J, Rui X, Qing G. Cytosolic DNA-STING-NLRP3 axis is involved in murine acute lung injury induced by lipopolysaccharide. Clin Transl Med. 2020;10:e228.
21. Joshi JC, Joshi B, Rochford I, Rayees S, Akhter MZ, Baweja S, et al. SPHK2-generated S1P in CD11b^{+} macrophages blocks STING to suppress the inflammatory function of alveolar macrophages. Cell Rep. 2020;30(4096-109):e5.
22. Huang LS, Hong Z, Wu W, Xiong S, Zhong M, Gao X, et al. mtDNA activates cGAS signaling and suppresses the YAP-mediated endothelial cell proliferation program to promote inflammatory injury. Immunity. 2020;52(475-86):e5.
23. Haag SM, Gulen MF, Reymond L, Gibelin A, Abrami L, Decout A, et al. Targeting STING with covalent small-molecule inhibitors. Nature. 2018;559:269–73.
24. Shao J, Stout I, Volger OL, Hendriksen PJ, van Loveren H, Peijnenburg AA. Inhibition of CXCL12-mediated chemotaxis of Jurkat cells by direct immunotoxicants. Arch Toxicol. 2016;90:1685–94.
25. de Souza Xavier Costa N, Ribeiro Júnior G, Dos Santos Alemany AA, Belotti L, Zati DH, Frota Cavalcante M, et al. Early and late pulmonary effects of nebulized LPS in mice: An acute lung injury model. PLoS One. 2017;12:e0185474.
26. Schingnitz U, Hartmann K, Macmanus CF, Eckle T, Zug S, Colgan SP, et al. Signaling through the A2B adenosine receptor dampens endotoxin-induced acute lung injury. J Immunol. 2010;184:5271–9.
27. Kim JJ, Shajib MS, Manocha MM, Khan WI. Investigating intestinal inflammation in DSS-induced model of IBD. J Visual Exp. 2012;60:e3678.
28. Wu Y, Wu B, Zhang Z, Lu H, Fan C, Qi Q, et al. Heme protects intestinal mucosal barrier in DSS-induced colitis through regulating macrophage polarization in both HO-1-dependent and HO-1-independent way. FASEB J. 2020;34:8028–43.
29. Kitada S, Kayama H, Okuzaki D, Koga R, Kobayashi M, Arima Y, et al. BATF2 inhibits immunopathological Th17 responses by suppressing Il23a expression during *Trypanosoma cruzi* infection. J Exp Med. 2017;214:1313–31.
30. Domenici-Lombardo L, Adembri C, Consalvo M, Forzini R, Meucci M, Romagnoli P, et al. Evolution of endotoxin induced acute lung injury in the rat. Int J Exp Pathol. 1995;76:381–90.
31. Patel BV, Wilson MR, Takata M. Eur Respir J. 2012;39:1162–70.
32. Matthay MA, Zemans RL. The acute respiratory distress syndrome: pathogenesis and treatment. Annu Rev Pathol. 2011;6:147–63.
33. Zhao Q, Wei Y, Pandol SJ, Li L, Habtezion A. STING signaling promotes inflammation in experimental acute pancreatitis. Gastroenterology. 2018;154:1822–35.e2.
34. Petrasek J, Iracheta-Vellve A, Csak T, Satishchandran A, Kodys K, Kurt-Jones EA, et al. STING-IRF3 pathway links endoplasmic reticulum stress with hepatocyte apoptosis in early alcoholic liver disease. Proc Natl Acad Sci USA. 2013;110:16544–9.
35. Maekawa H, Inoue T, Ouchi H, Jao TM, Inoue R, Nishi H, et al. Mitochondrial damage causes inflammation via cGAS-STING signaling in acute kidney injury. Cell Rep. 2019;29:1261–73.e6.
36. Yu Y, Liu Y, An W, Song J, Zhang Y, Zhao X. STING-mediated inflammation in Kupffer cells contributes to progression of nonalcoholic steatohepatitis. J Clin Invest. 2019;129:546–55.
37. Li N, Zhou H, Wu H, Wu Q, Duan M, Deng W, et al. STING-IRF3 contributes to lipopolysaccharide-induced cardiac dysfunction, inflammation, apoptosis and pyroptosis by activating NLRP3. Redox Biol. 2019;24:101215.
38. Peng Y, Zhuang J, Ying G, Zeng H, Zhou H, Cao Y, et al. Stimulator of IFN genes mediates neuroinflammatory injury by suppressing AMPK signal in experimental subarachnoid hemorrhage. J Neuroinflammation. 2020;17:165.
39. Maekawa H, Inoue T, Ouchi H, Jao TM, Inoue R, Nishi H, et al. Mitochondrial damage causes inflammation via cGAS-STING signaling in acute kidney injury. Cell Rep. 2019;29:1261–73 e6.
40. Grommes J, Soehnlein O. Contribution of neutrophils to acute lung injury. Mol Med. 2011;17:293–307.
41. Abraham E. Neutrophils and acute lung injury. Crit Care Med. 2003;31:S195–9.
42. Liu L, Mao Y, Xu B, Zhang X, Fang C, Ma Y, et al. Induction of neutrophil extracellular traps during tissue injury: Involvement of STING and Toll-like receptor 9 pathways. Cell Prolif. 2019;52:e12579.

43. Muller WA. Leukocyte-endothelial-cell interactions in leukocyte transmigration and the inflammatory response. Trends Immunol. 2003;24:327–34.
44. Sato T, Shibata W, Maeda S. Adhesion molecules and pancreatitis. J Gastroenterol. 2019;54:99–107.
45. Singh S, Anshita D, Ravichandiran V. MCP-1: Function, regulation, and involvement in disease. Int Immunopharmacol. 2021;107598. https://doi.org/10.1016/j.intimp.2021.107598.
46. Petrovic-Djergovic D, Popovic M, Chittiprol S, Cortado H, Ransom RF, Partida-Sánchez S. CXCL10 induces the recruitment of monocyte-derived macrophages into kidney, which aggravate puromycin aminonucleoside nephrosis. Clin Exp Immunol. 2015;180:305–15.
47. Larsen JM. The immune response to *Prevotella bacteria* in chronic inflammatory disease. Immunology. 2017;151:363–74.
48. Kitajima S, Ivanova E, Guo S, Yoshida R, Campisi M, Sundararaman SK, et al. Suppression of STING associated with LKB1 loss in KRAS-driven lung cancer. Cancer Discov. 2019;9:34–45.
49. Liu Y, Jesus AA, Marrero B, Yang D, Ramsey SE, Sanchez GAM, et al. Activated STING in a vascular and pulmonary syndrome. N Engl J Med. 2014;371:507–18.